

LETTER

Pb-free perovskite solar cells composed of Sn/Ge(1:1) alloyed perovskite layer prepared by spin-coating

To cite this article: Huan Bi *et al* 2023 *Appl. Phys. Express* **16** 036501

View the [article online](#) for updates and enhancements.

You may also like

- [Epitaxial Growth of Mirror Smooth Ge on GaAs and Ge by the Low Temperature Ge₂ Disproportionate Reaction](#)
M. Berkenblit, A. Reisman and T. B. Light
- [Gaseous Equilibria in the Germanium Iodine System](#)
R. F. Lever
- [Epitaxial Growth of Germanium by the Hydrogen Reduction of GeI₄](#)
Shinya Iida



Pb-free perovskite solar cells composed of Sn/Ge(1:1) alloyed perovskite layer prepared by spin-coating

Huan Bi^{*}, Mengmeng Chen, Liang Wang, Zheng Zhang, Chao Ding, Gaurav Kapil, Shahrir Razey Sahamir, Yoshitaka Sanehira, Ajay Kumar Baranwal, Takeshi Kitamura, Guozheng Shi, Qing Shen^{*}, and Shuzi Hayase^{*}

Faculty of Informatics and Engineering, The University of Electro-Communications, 1-5-1 Chofugaoka, Chofu, Tokyo 182-8585, Japan

^{*}E-mail: hbi.trans.sci@uec.ac.jp; shen@pc.uec.ac.jp; hayase@uec.ac.jp

Received January 18, 2023; revised February 13, 2023; accepted February 24, 2023; published online March 10, 2023

Since the DMSO seriously oxidizes the GeI₂ which is one of the ingredients for the Sn/Ge perovskite, it was difficult to make high-quality films by using the conventional DMSO/DMF solvent. We now first report the MASn_{0.5}Ge_{0.5}I₃ perovskite solar cells (PSCs) prepared by a simple spin-coating technology. We found that triethanolamine (TEA)/*n*-methyl pyrrolidone (NMP) does not oxidize the GeI₂ and improves the stability of the precursor. The precursor solution with TEA/NMP/DMF gave high-quality perovskite films. The cell gave a power conversion efficiency of 2.18%. This is the first report proving that Sn/Ge PSCs are fabricated by a conventional solution process. © 2023 The Japan Society of Applied Physics

Supplementary material for this article is available [online](#)

The efficiency of the lead halide perovskite solar cells (Pb PSCs) has been improved and reached 25.7%.¹ There is tin (Sn) and germanium (Ge) in the same 14th group as the lead. The tin halide perovskite solar cells (Sn PSCs) are now following the Pb PVK and 14%–15% efficiency has been reported.² On the other hand, fundamental research such as the electronic and optical properties of the germanium halide perovskite (Ge-PVK) layer have been reported, however, the efficiency of the Ge PSCs is lower than the above.³ In addition to the halide perovskite solar cells with single metal cations such as Pb PVK PSCs, Sn PVK PSCs, and Ge-PVK PSCs, alloyed perovskite solar cells consisting of more than two metal cations, have attracted attention due to the unique solar cell performances.⁴ The bandgap of the Pb PVK and Sn PVK is around 1.55–1.6 eV and 1.4 eV, respectively.^{5,6} However, the bandgap of the Sn/Pb alloyed perovskite is around 1.2 eV,⁷ which is much narrower than that of each perovskite. The efficiency of the Sn/Pb PVK PSCs has been improved and 23%–24% efficiency has been reported.^{7,8} The Sn/Pb PVK PSCs are expected as the bottom cell of all perovskite/perovskite tandem solar cells.^{9,10}

The results on the Sn/Pb PVK PSCs stimulated us to research alloyed perovskite Sn/Ge alloyed halide perovskite solar cells (Sn/Ge-PVK PSCs), where both of Sn and Ge are in neighbors of the 14th group in the periodic table, such as Sn/Pb PVK PSCs. The Sn/Ge-PVK layer is fabricated from SnI₂, GeI₂, and organic halides (A-halides) in ASn_xGe_(1-x)I₃. It is well-known that dimethyl sulfoxide/dimethylformamide (DMSO/DMF) mixture solvent is employed to make high-quality halide perovskite films.^{11–13} The use of DMSO was unavoidable because the DMSO makes intercalated precursor (2D structure) with PbI₂ or SnI₂, and the 2D structure is converted to the 3D structure with high-quality films.^{12,13} Since GeI₂ is a strong reducing agent and reacts with DMSO (oxidant), the DMSO is not employed for preparing the Sn/Ge-PVK layer.^{14–16} Therefore, in order to fabricate the Sn/Ge alloyed halide perovskite (Sn/Ge-PVK) layers, a vacuum deposition process or specially designed spray method (DMF solution) has been used.³ We have reported that the efficiency of the Sn PVK PSCs was enhanced by adding a small amount of GeI₂ (such as Sn/Ge-PVK PSCs consisting of Sn_{0.95}Ge_{0.05} PVK as the light-harvesting layer).^{17,18} The

addition of GeI₂ toward SnI₂ was limited to 10% in the process using the DMF/DMSO mixed solvent, because of the low solubility of GeI₂ and the high reactivity of the GeI₂ with DMSO.^{3,19} Because of this, there were no reports on the Sn/Ge-PVK PSCs prepared by a conventional coating technology. We found that triethanolamine (TEA)/*n*-methyl pyrrolidone (NMP) solves these problems. This is the first report on the Sn/Ge-PVK PSCs [MASn_{0.5}Ge_{0.5}I₃ (MA: CH₃NH₃⁺)] prepared by a simple spin-coating technology. The results open the way toward printable Pb-free Sn/Ge PSCs.

We first used DMF/NMP (4:1, V:V) and DMF/DMSO (4:1, V:V) as a solvent to prepare MASn_{0.5}Ge_{0.5}I₃ perovskite film. As shown in Fig. S1, no matter which strategy was used, films with good quality were not obtained. It has been reported that Ag⁺ is reduced to Ag metal in the presence of TEA.^{20,21} In addition, the amine groups coordinate with Sn²⁺ or Ge²⁺, which retards the crystallization and gives better crystals.^{22–24} This prompted us to add TEA instead of DMSO. Figures 1(a)–1(b) shows the ultraviolet–visible (UV–vis) spectra change during the storage of SnI₂ in DMF/NMP/DMSO (4:1:0.5, volume, hereinafter referred to as DMSO solution) and DMF/NMP/TEA (4:1:0.25, volume, hereinafter referred to as TEA solution), respectively. The change of the UV–vis spectra of SnI₂ in the DMSO solution was larger than that in the TEA solution. The absorption at around 360 nm is assigned to I₃[−] which is formed by the oxidation of the SnI₂.²⁵ Therefore, the 360 nm peak was taken as the indicator for the SnI₂ stability. Figure S2 summarizes the relationship between the change of 360 nm peak intensity and the elapsed time for each solution. The peak intensity change of 360 nm was suppressed in the TEA solution, suggesting that the stability of the SnI₂ was improved in the TEA solution. Figures 1(c)–1(d) shows the UV–vis spectra change of GeI₂ in the DMSO solution and TEA solution, respectively. In the same way, the UV–vis spectra change was more suppressed in the TEA solution.

XRD spectra of MASn_xGe_(1-x)I₃ are summarized in Fig. 2. MASn_xGe_(1-x)I₃ prepared from DMSO solvent (Sn_xGe_(1-x)-DMSO solution) had a lot of unidentified peaks [Fig. 2(a)]. In contrast to this, MASn_xGe_(1-x)I₃ prepared from TEA (Sn_xGe_(1-x)-TEA solution, Fig. 2(b)) shows simple XRD peaks at 14.83° and 29.22° assigned to the (001) and

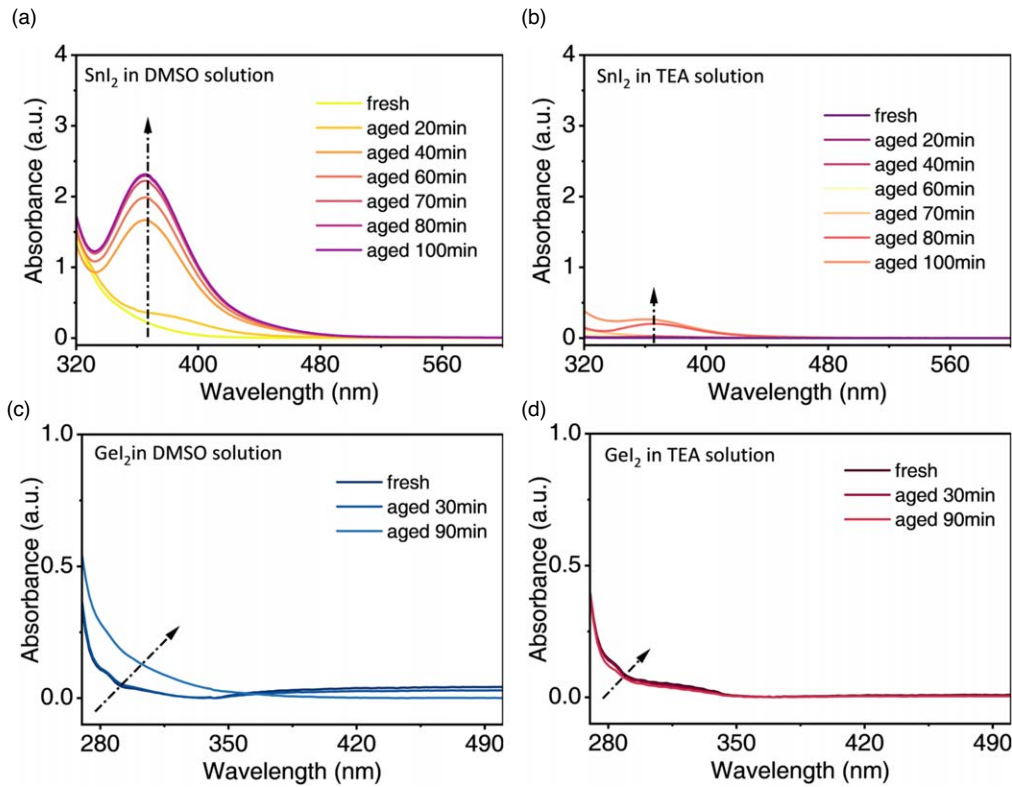


Fig. 1. (Color online) UV-vis spectrum changes of SnI_2 dissolved in (a) DMSO solution, and (b) TEA solution. UV-vis spectrum changes of GeI_2 dissolved in (c) DMSO solution, and (d) TEA solution.

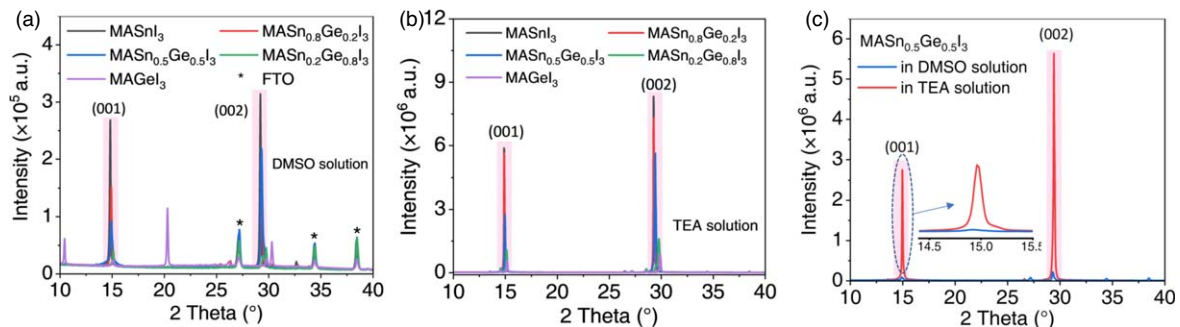


Fig. 2. (Color online) XRD patterns of the perovskite film ($\text{MASn}_x\text{Ge}_{1-x}\text{I}_3$) prepared from (a) DMSO solution and (b) TEA solution. (c) XRD patterns of $\text{MASn}_{0.5}\text{Ge}_{0.5}\text{I}_3$ perovskite film prepared from DMSO solution and TEA solution.

(002) for each composition ($x = 1-0$). The results demonstrate strongly that the latter crystal has a more regulated structure than the former crystal and prove the effectiveness of the TEA solution. The peak shifted to a larger degree with a decrease in the x of $\text{MASn}_x\text{Ge}_{1-x}\text{I}_3$ (Figs. S3 and S4), suggesting that the lattice becomes smaller as the Ge^{2+} ion content increases because the diameter of Ge^{2+} ion is smaller than that of the Sn^{2+} ion. These results show that the Ge^{2+} is in the lattice. In addition, it has been reported that the small XRD intensity is associated with poor crystallization.²⁶⁻³⁰ The poor crystallization quality of the film may be explained by the faster crystallization rate of the film with the increase of Ge^{2+} . This is also a challenge for preparing high Ge^{2+} PSCs [Figs. 3(c) and S3]. In addition, full width at half maximum (FWHM) was also counted to uncover the effect of TEA or DMSO on the crystallinity of the perovskite film. The FWHM of the $\text{MASn}_x\text{Ge}_{1-x}\text{I}_3$ film prepared from the precursor solution containing TEA is always smaller than that of the film prepared from the precursor solution

containing DMSO (Fig. S5), which supports that the quality of the perovskite film prepared from the former precursor is better.

The morphology of the crystal surface of $\text{MASn}_{0.5}\text{Ge}_{0.5}\text{I}_3$ prepared from TEA solution was pinhole free and improved, compared with that from DMSO solution. Video S1 and Video S2 show the spin-coating process. In the case of perovskite film prepared from the DMF/NMP solution (Video S1), the black film appeared in 7 s after the spin-coating, while for the perovskite film from TEA solution (Video S2), the black film appeared at 10.5 s after the spin-coating. The slower crystallization may explain the better film morphology as reported previously.^{22,31}

The $\text{Sn}^{4+}/\text{Sn}^{2+}$ ratio of the perovskite film ($\text{MASn}_{0.5}\text{Ge}_{0.5}\text{I}_3$) prepared from the DMSO solution and TEA solution are summarized in Fig. 3. The ratio was $\text{Sn}^{2+}:\text{Sn}^{4+} = 100:0$ in the latter film (TEA solution), which was lower than that in the former film prepared from DMSO solution ($\text{Sn}^{2+}:\text{Sn}^{4+} = 92:8$) as shown in Figs. 3(a)-3(b). In

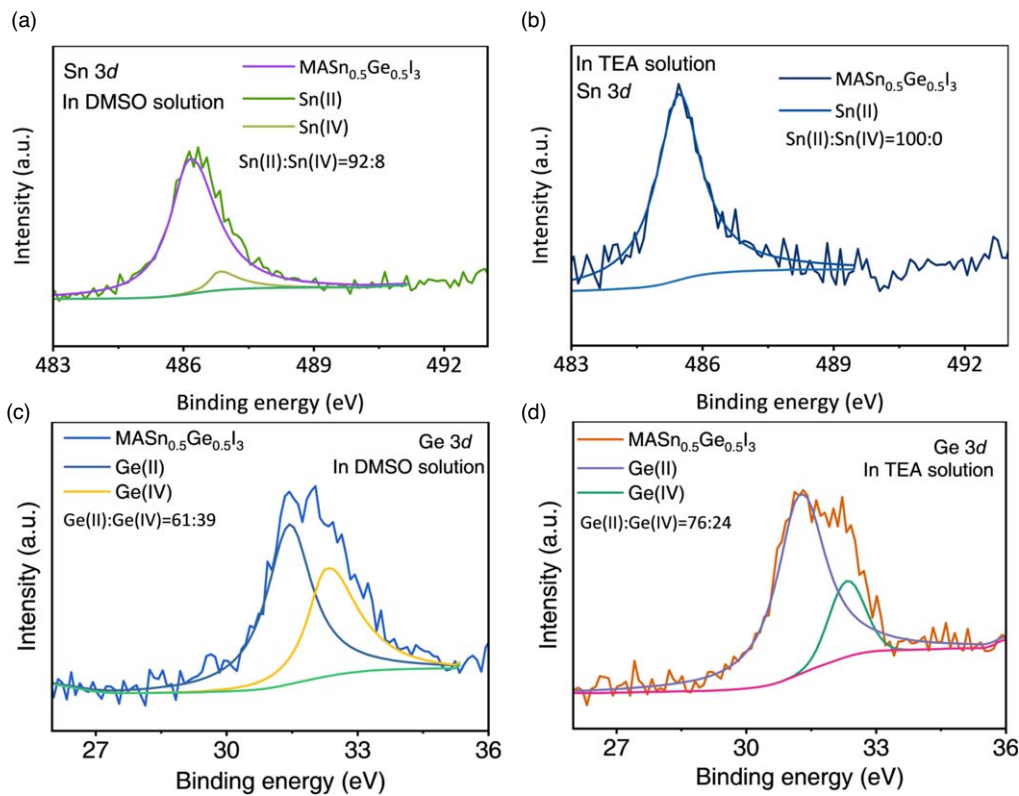


Fig. 3. (Color online) Ge 3d XPS spectra of $\text{MASn}_{0.5}\text{Ge}_{0.5}\text{I}_3$ fabricated from the (a) DMSO solution and (b) TEA solution. Sn 3d XPS of $\text{MASn}_{0.5}\text{Ge}_{0.5}\text{I}_3$ fabricated from the (c) DMSO solution and (d) TEA solution.

the same way, the $\text{Ge}^{2+}/\text{Ge}^{4+}$ ratio was $\text{Ge}^{2+}:\text{Ge}^{4+} = 76:24$ in the latter film (prepared from TEA solution) [Figs. 3(c)–3(d)], which was lower than in the former film ($\text{Ge}^{2+}:\text{Ge}^{4+} = 61:39$, prepared from DMSO solution). These results show that the Sn^{4+} and Ge^{4+} formation was retarded in the TEA solution.

Figure 4(a) shows the photovoltaic performances of perovskite solar cells having the perovskite layer ($\text{MASn}_{0.5}\text{Ge}_{0.5}\text{I}_3$) prepared from DMSO (device 1) solution with the anti-solvent process and TEA solution (device 2) without anti-solvent process, where the former device and the latter device is named as device 1 and device 2 respectively. The device has a structure of FTO/PEDOT:PSS/ $\text{MASn}_{0.5}\text{Ge}_{0.5}\text{I}_3$ /C60/BCP/Ag. The $\text{MASn}_{0.5}\text{Ge}_{0.5}\text{I}_3$ layer was prepared by spin-coating from TEA solution without the anti-solvent process. The $\text{MASn}_{0.5}\text{Ge}_{0.5}\text{I}_3$ layer was not prepared from the conventional DMF/DMSO (4:1) solution because of the inadequate solubility and the fast reactivity of the DMSO with GeI_2 . Because of this, the content of DMSO was decreased to DMF/DMSO (4:0.5, V:V). Since the solution did not give a flat film after the spin-coating, an anti-solvent process was employed after the spin-coating. Figure 4(b) and Table SI present the J - V curves and photovoltaic parameters of the champion PSCs prepared from $\text{Sn}_{0.5}\text{Ge}_{0.5}$ -DMSO (device 1) with the anti-solvent process and $\text{Sn}_{0.5}\text{Ge}_{0.5}$ -TEA without anti-solvent process (device 2), respectively. The former device (device 1) had PCE of 1.36%, J_{SC} of 10.15 mA cm^{-2} , V_{OC} of 0.28 V, and FF of 0.48. While the latter device (device 2) achieved PCE of 2.18%, J_{SC} of 11.04 mA cm^{-2} , V_{OC} of 0.38 V, and FF of 0.53. The energy diagram of the solar cells is shown in Fig. S6. The conduction band energy level and balance band

energy level were -3.75 eV and -5.40 eV , respectively, where electrons and holes can be collected from the viewpoint of the energy level. There was no difference in the conduction and valence band energy levels between the film prepared from $\text{Sn}_{0.5}\text{Ge}_{0.5}$ -DMSO with an anti-solvent process and that from $\text{Sn}_{0.5}\text{Ge}_{0.5}$ -TEA without an anti-solvent process. The incident photon-to-current conversion efficiency (IPCE) spectra of device 2 were shown in Fig. 4(c). The current density was estimated to be 10.22 mA cm^{-2} which agreed with the J_{SC} in J - V curves. The stable PCE of device 2 is shown in Fig. S7. The PCE of 1.88% and 9.8 mA cm^{-2} of device 2 was kept for 150 s. Figure 4(d) shows the stability test results of the unencapsulated device 2 in the N_2 atmosphere. After 500 h, 97.1% of its original PCE was maintained.

The $\text{MASn}_{0.5}\text{Ge}_{0.5}\text{I}_3$, where the content of Ge^{2+} is much higher than Ge^{2+} -doped tin perovskite solar cells previously reported by us, was difficult to prepare by spin-coating technology from the conventionally employed DMF/DMSO (4:1) solvent, because of the small solubility and instability of the Sn/Ge perovskite. It was proved that the Sn/Ge alloyed perovskite layer was prepared from DMF/NMP/TEA (4:1:0.25) solution by a spin-coated method and without the anti-solvent process for the first time. The use of TEA in DMF retarded the oxidation of Sn^{2+} and Ge^{2+} . Our results open the way to Pb-free Sn/Ge alloyed perovskite solar cells prepared by coating technologies such as spin-coating and blade coating.

Acknowledgments We acknowledge financial support from JST-Mirai Program (JPMJMI22E2) and NEDO project on international collaboration. We also thank NEDO.

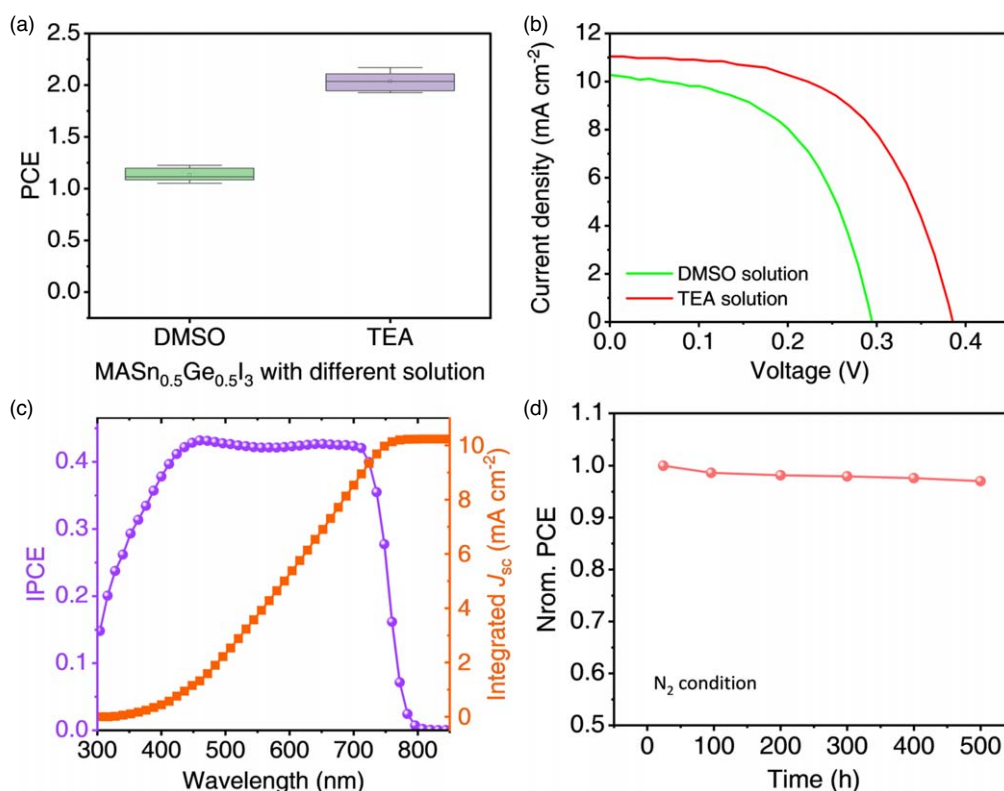


Fig. 4. (Color online) (a) Statistics of PCE of PSCs prepared from DMSO solution (device 1) and TEA solution (device 2); (b) *J*-*V* curves of the champion device 1 and device 2. (c) IPCE spectra of the champion device 2. (d) PCE change of device 2 aged in the glovebox filled with nitrogen.

ORCID iDs Huan Bi  <https://orcid.org/0000-0001-7680-9816>
 Yoshitaka Sanehira  <https://orcid.org/0000-0003-2030-2690>

- 1) "National Renewable Energy Laboratory (NREL)," Best Research-Cell Efficiency Chart, 2022 <https://nrel.gov/pv/cell-efficiency.html> (accessed 2022-10-18).
- 2) J. Cao and F. Yan, *Energy Environ. Sci.* **14**, 1286 (2021).
- 3) M. Chen et al., *Nat. Commun.* **10**, 16 (2019).
- 4) H. Bi, G. Han, M. Guo, C. Ding, S. Hayase, H. Zou, Q. Shen, Y. Guo, and W. Hou, *Sol. RRL* **2200352** (2022).
- 5) Z. Zhang et al., *Sol. RRL* **5**, 2100633 (2021).
- 6) F. Zhang, S. Ye, H. Zhang, F. Zhou, Y. Hao, H. Cai, J. Song, and J. Qu, *Nano Energy* **89**, 106370 (2021).
- 7) G. Kapil et al., *ACS Energy Lett.* **7**, 966 (2022).
- 8) S. Hu et al., *Energy Environ. Sci.* **15**, 2096 (2022).
- 9) W. Chen et al., *Nat. Energy* **7**, 229 (2022).
- 10) K. Xiao et al., *Nat. Energy* **5**, 870 (2020).
- 11) G. Nasti et al., *ACS Energy Lett.* **7**, 3197 (2022).
- 12) X. Jiang et al., *J. Am. Chem. Soc.* **143**, 10970 (2021).
- 13) Y. Zhang et al., *Adv. Energy Mater.* **10**, 2001300 (2020).
- 14) R. Chebolu, A. Bahuguna, R. Sharma, V. K. Mishra, and P. C. Ravikumar, *Chem. Commun.* **51**, 15438 (2015).
- 15) J. J. Wu, M. Muruganandham, J. S. Yang, and S. S. Lin, *Catal. Commun.* **7**, 901 (2006).
- 16) S. A. U. Hasan, D. S. Lee, S. H. Im, and K.-H. Hong, *Sol. RRL* **4**, 1900310 (2020).
- 17) F. Liu et al., *Chem. Mater.* **31**, 798 (2019).
- 18) C. H. Ng et al., *Nano Energy* **58**, 130 (2019).
- 19) M. Chen, Q. Dong, C. Xiao, X. Zheng, Z. Dai, Y. Shi, J. M. Luther, and N. P. Padture, *ACS Energy Lett.* **7**, 2256 (2022).
- 20) Y. Liu, M. Gao, L. Zheng, J. Zhao, H. Wang, K. Han, and Y. Zhou, *Colloids Surf. A Physicochem. Eng. Asp.* **567**, 96 (2019).
- 21) Z. Jia, H. Sun, and Q. Gu, *Colloids Surf. A Physicochem. Eng. Asp.* **419**, 174 (2013).
- 22) C.-M. Tsai, G.-W. Wu, S. Narra, H.-M. Chang, N. Mohanta, H.-P. Wu, C.-L. Wang, and E. W.-G. Diau, *J. Mater. Chem. A* **5**, 739 (2017).
- 23) T. Mahmoudi, M. Kohan, W.-Y. Rho, Y. Wang, Y. H. Im, and Y.-B. Hahn, *Adv. Energy Mater.* **12**, 2201977 (2022).
- 24) F. Wang, H. Yu, H. Xu, and N. Zhao, *Adv. Funct. Mater.* **25**, 1120 (2015).
- 25) B. Li, F. H. Isikgor, H. Coskun, and J. Ouyang, *Angew. Chem. Int. Ed.* **56**, 16073 (2017).
- 26) A. A. Ramadan, A. A. Abd El-Mongy, A. M. El-Shabiny, A. T. Mater, S. H. Mostafa, E. A. El-Sheehedy, and H. M. Hashem, *Cryst. Res. Technol.* **44**, 111 (2009).
- 27) E. Jokar, C.-H. Chien, A. Fathi, M. Rameez, Y.-H. Chang, and E. W.-G. Diau, *Energy Environ. Sci.* **11**, 2353 (2018).
- 28) F. Xie, C.-C. Chen, Y. Wu, X. Li, M. Cai, X. Liu, X. Yang, and L. Han, *Energy Environ. Sci.* **10**, 1942 (2017).
- 29) H. Sohrabpoor, M. Elyasi, M. Aldosari, and N. E. Gorji, *Superlattices Microstruct.* **97**, 556 (2016).
- 30) P. Wang, J. Wang, X. Zhang, H. Wang, X. Cui, S. Yuan, H. Lu, L. Tu, Y. Zhan, and L. Zheng, *J. Mater. Chem. A* **6**, 15853 (2018).
- 31) X. Meng, J. Lin, X. Liu, X. He, Y. Wang, T. Noda, T. Wu, X. Yang, and L. Han, *Adv. Mater.* **31**, 1903721 (2019).